

Figure S1

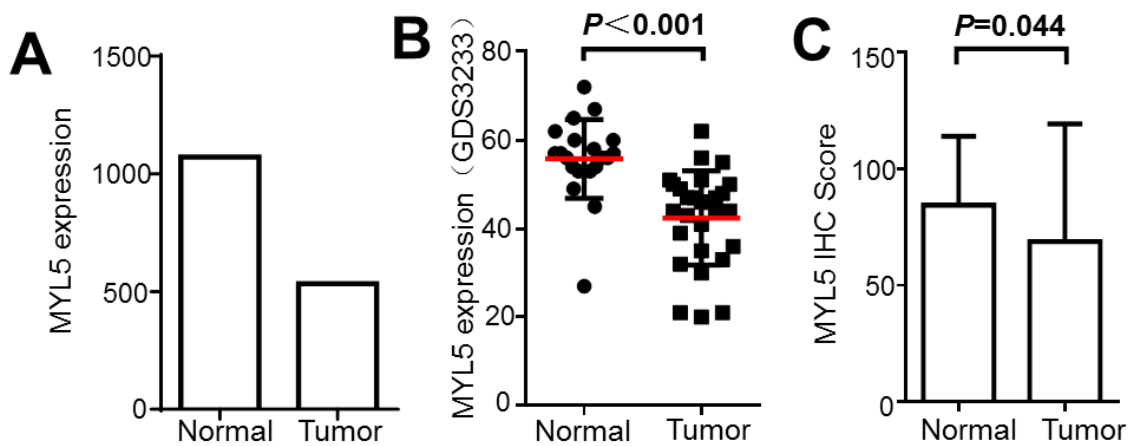


Figure S1. Expression of MYL5 in cervical cancer. A. Mean intensity of MYL5 in cervical normal and tumor tissues detected by gene microarray. B. Expression analysis of MYL5 cervical normal and tumor tissues based on the data of NCBI/GEO DataSets/GDS3233. C. Immunochemical staining confirms MYL5 decreased in tumor tissues from 58 paired early stage samples.

Figure S2

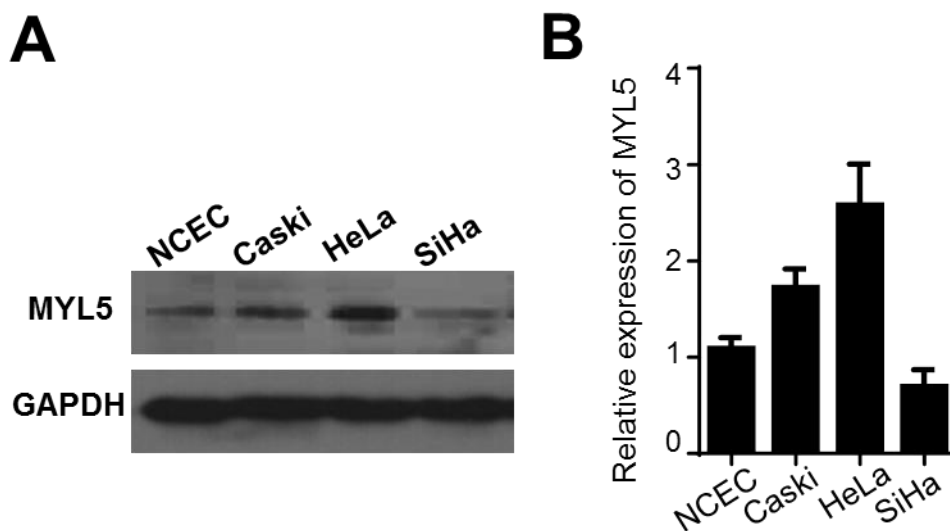


Figure S2. Expression of MYL5 in cervical cancer cells. A. Western blot analyses of MYL5 in normal human cervical epithelial cells (NCEC) and cervical cancer cell lines. B. Quantitative RT-PCR analyses of MYL5 in cervical cells.

Figure S3

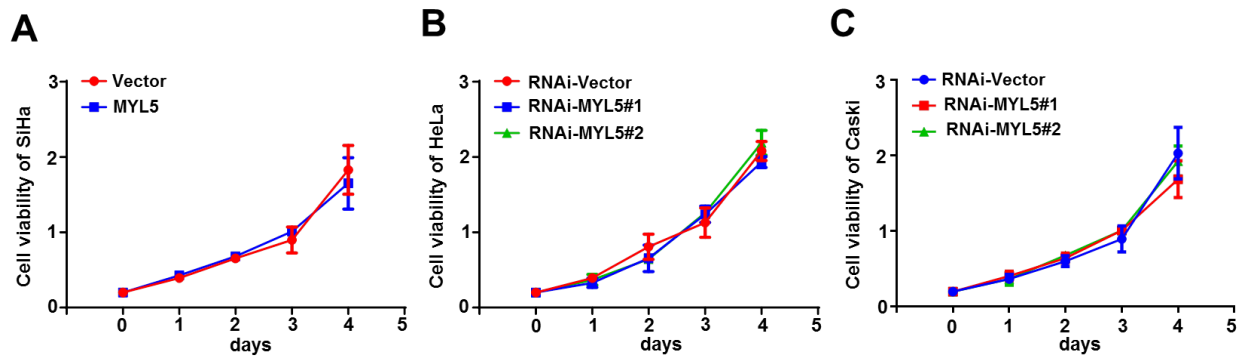


Figure S3. MYL5 did not affect the growth of cervical cancer cells. Cell viability of SiHa (A), HeLa (B), and Caski (C) were analysed by MTS assay. The dot represent the means, and the bars indicate the s.e.m. The results are expressed as mean \pm s.e.m. of 3 independent experiments.

Figure S4

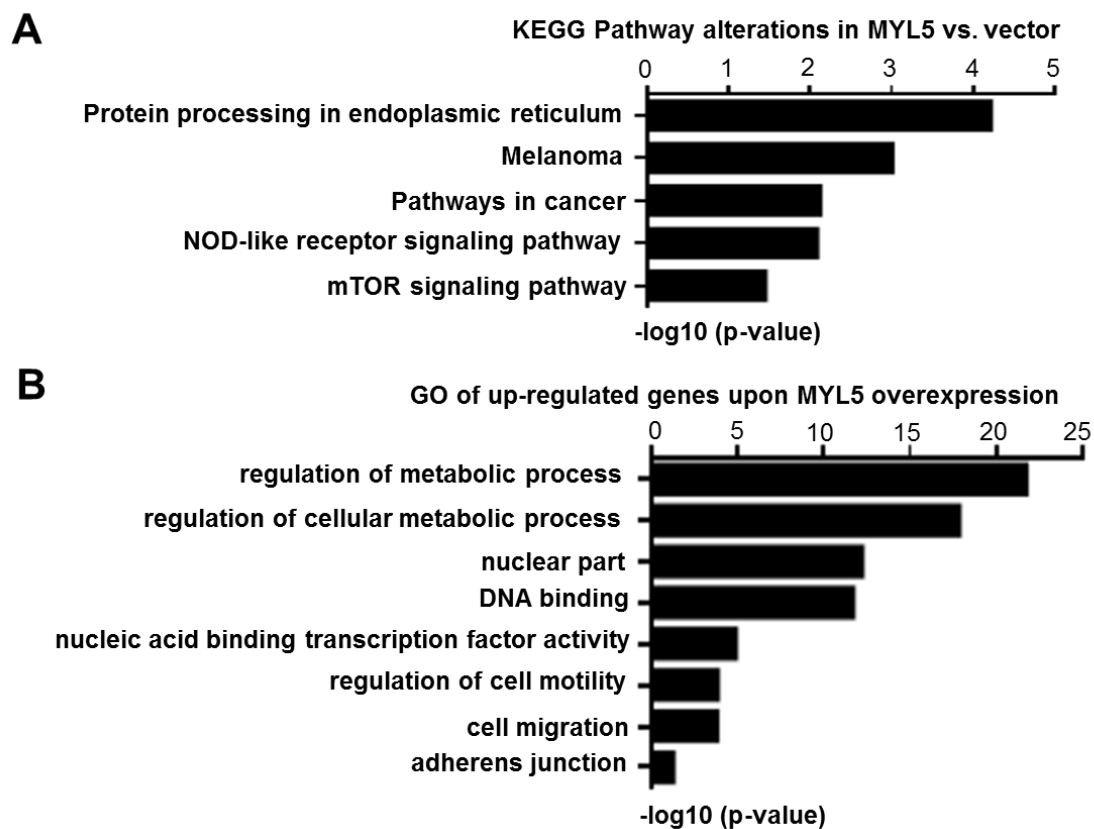


Figure S4. KEGG pathway and GO analysis of genes up-regulated upon MYL5 overexpression. KEGG (Kyoto Encyclopedia of Genes and Genomes) pathway (A) and GO (gene ontology) analysis (B) of genes up-regulated upon MYL5 overexpression, using the gene annotation tool from the DAVID database. Black bars represent the $-\log_{10}$ of p-values of each category.

Figure S5

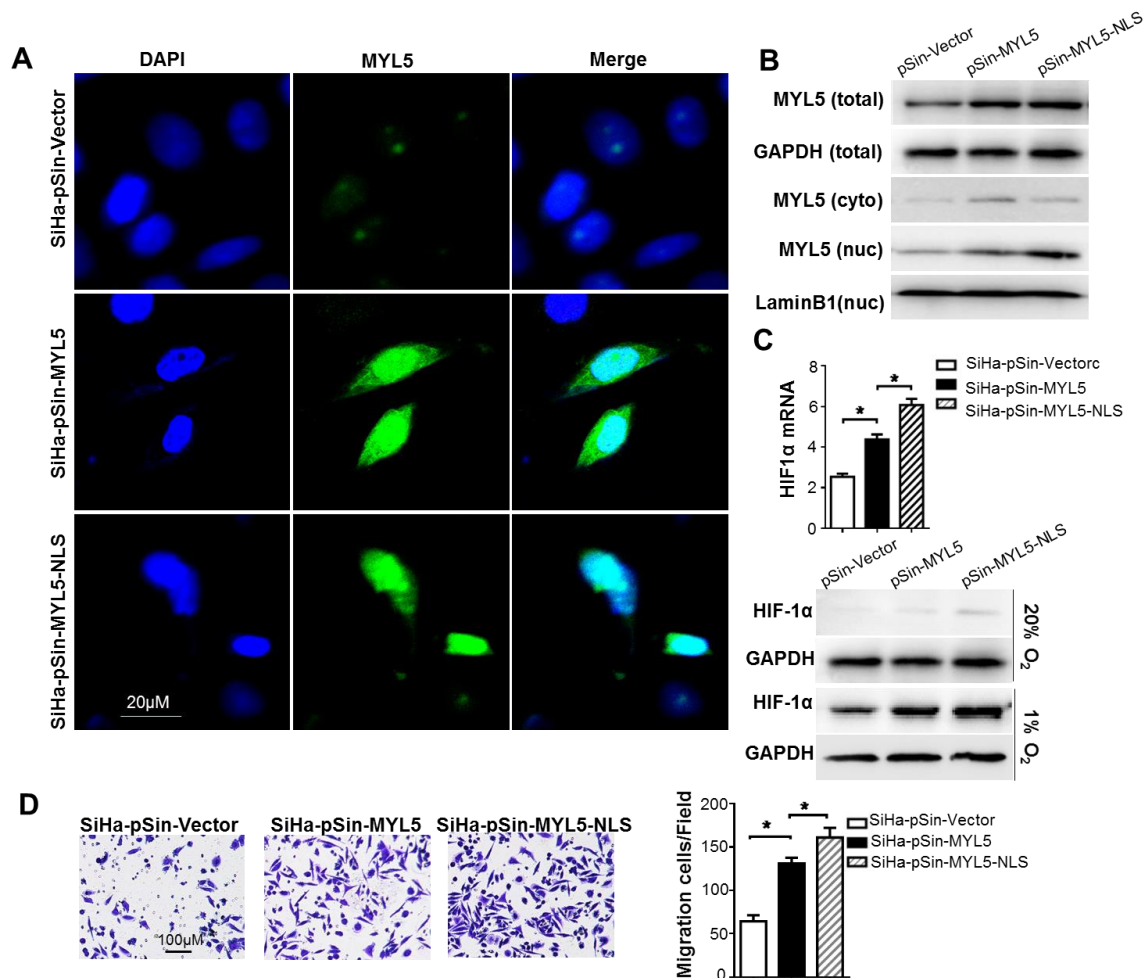


Figure S5. Overexpression of MYL5 with NLS further increases HIF-1 α expression and cell migration ability. **A.** Immunofluorescence images of MYL5 (green) in indicated SiHa cells. Merged images represent overlays of MYL5 (green) and nuclear staining by DAPI (blue). Bar=20 μ m. **B.** Western blots of total, cytoplasmic (cyto) and nuclear (nuc) MYL5 in the indicated cells. Total control, GAPDH; nuclear control, Lamin B1. **C.** Quantitative RT-PCR and western blot analyses of HIF-1 α expression in the indicated cells. **D.** Overexpression of MYL5 with NLS promotes SiHa cell migration further. The data represented are shown as mean \pm s.e.m. collected from 6 fields of 3 independent experiments.

Bar=100 μ m. * P <0.05 by Student's t-test.

Figure S6

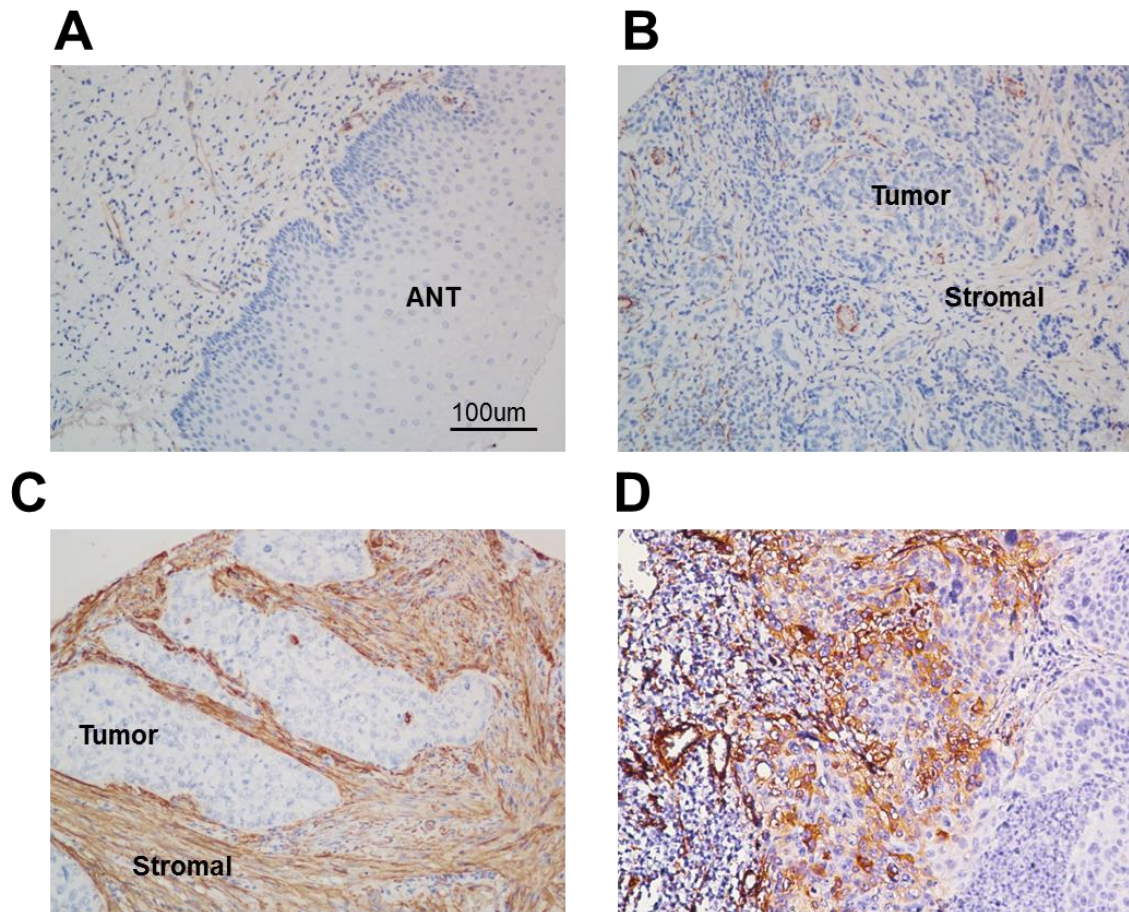


Figure S6. Representative images of MYL9 staining in cervical cancer tissues. A. Immunohistochemistry staining of MYL9 in cervical adjacent noncancerous tissue (ANT). **B.C. D.** The staining of MYL9 in tumor tissues and stroma tissues.

Figure S7

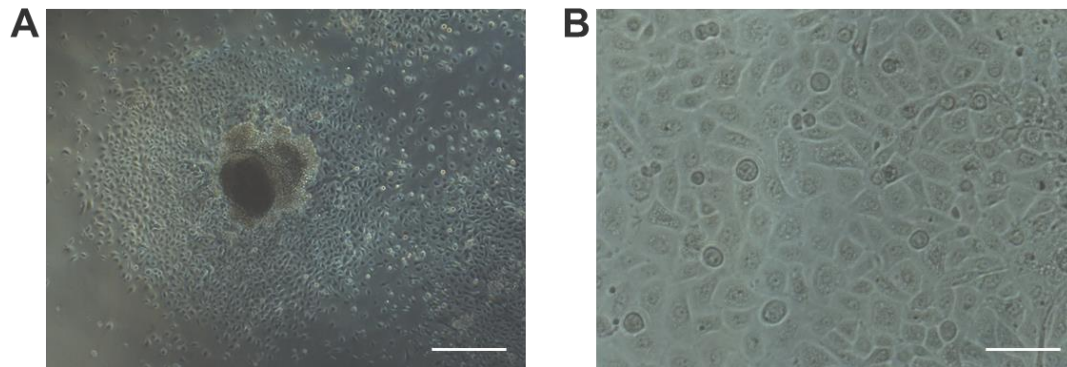


Figure S7. Representative images of primary normal cervical epithelial cells (NCECs). A. NCECs observed on the fifth day in lower power field. Bar=500 μ m. **B.** NCECs observed in high power field. Bar=50 μ m.

Figure S8

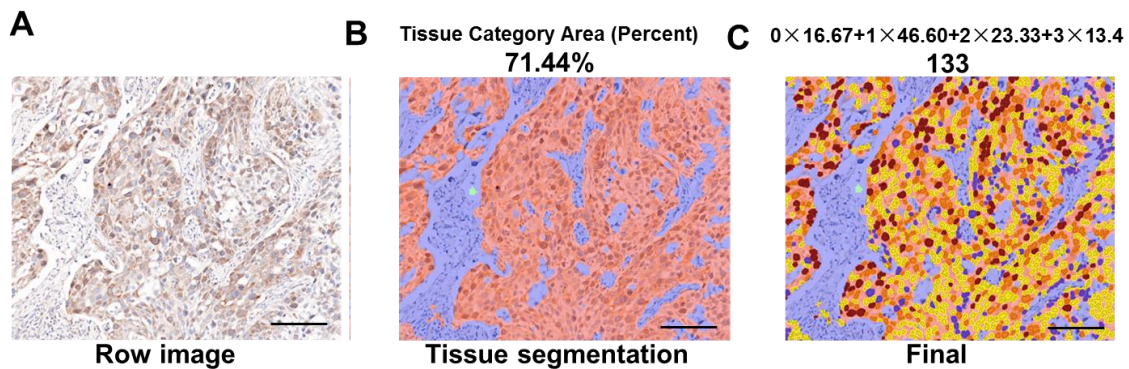


Figure S8. Details of automated quantification method for immunohistochemistry staining. A. Raw image acquired using the 20 \times objective lens on the Vectra scanner. **B.** Representative compartment image following automated segmentation. **C.** Final composite image of the automated tissue and object segmentation. Bar=100 μ m.

Table S1 Correlations between MYL5 expression and clinicopathological features of patients with cervical carcinoma

Characteristics	IHC data set (n=167) MYL5		P value
	Low	High	
<i>Age, years</i>			0.899
>35	96	35	
≤35	26	10	
<i>FIGO stage</i>			0.527
I	89	35	
II	33	10	
<i>Grade of differentiation</i>			0.78
1,2	49	17	
3	73	28	
<i>Greatest tumor dimension, cm</i>			0.203
>4cm	24	13	
≤4cm	98	32	
<i>Lymphovascular space invasion</i>			0.563
Yes	5	1	
No	117	44	
<i>Depth of cervical invasion</i>			0.834
≥ 66%	51	18	
<66%	71	27	
<i>Uterine corpus invasion</i>			0.498
Yes	9	2	
No	113	43	
<i>Pelvic lymph node metastasis</i>			0.025 ^a
Yes	19	14	
No	103	31	
<i>Distant metastasis and recurrence</i>			0.017 ^a
Yes	18	14	
No	104	31	

The Pearson chi-squared test and Fisher's exact test were used for analysis.

^a P-value with significance ($P < 0.05$).

Table S2 Primers for real-time PCR

Genes	Forward	Reverse
<i>β-actin</i>	5'-TCCCTGGAGAAGAGCTACGA-3'	5'-AGCACTGTGTTGGCGTACAG-3'
<i>GAPDH</i>	5'-CTCCTCCTGTTCGACAGTCAGC-3'	5'-CCCAATACGACCAAATCCGTT-3'
<i>HIF-1α</i>	5'-ATCCATGTGACCATGAGGAAATG-3'	5'-TCGGCTAGTTAGGGTACACTTC-3'
<i>MYL5</i>	5'-GCCGAGGAGACCATTCTTAACGC-3'	5'-TGGAGGCGAACTGGAACATCTGG-3'
<i>SNAI2</i>	5'-CTGGGCGCCCTGAACATGCAT-3'	5'-GGCTTCTCCCCCGTGTGAGTTCTA-3'
<i>ZEB1</i>	5'-AGTGGTCATGATGAAAATGGAACACCA-3'	5'-AGGTGTAACTGCACAGGGAGCA-3'
<i>GLUT1</i>	5'-TCTGGCATCAACGCTGTCTTC-3'	5'-CGATACCGGAGCCAATGGT-3'
<i>p21</i>	5'-TGTCCGTCAGAACCCATGC-3'	5'-AAAGTCGAAGTTCCATCGCTC-3'
<i>ENO1</i>	5'-CTGGTGCCGTTGAGAAGGG-3'	5'-GGTTGTGGTAAACCTCTGCTC-3'
<i>PKM2</i>	5'-ATGTCGAAGCCCCATAGTGAA-3'	5'-TGGGTGGTGAATCAATGTCCA-3'

Table S3 Antibodies for IHC, IF

Target protein	IHC	IF	WB	CHIP	Company and catalogue number
<i>MYL5</i>	1:150	1:50	1:500		Sigma-Aldrich,cat#HPA037381
<i>Flag</i>				1:50	Cell Signaling, cat#14793
<i>HIF-1α</i>	1:400		1:1000		Epitomics,cat#2015-01
<i>HIF-1α</i>				1:50	Cell Signaling, cat#14179
<i>Cytokeratin</i>	1:1				MXB, cat#MAB-0671
<i>GAPDH</i>			1:10,000		Abgent, cat#AP7873a
<i>LaminB1</i>			1:1000		KeyGen Biotech, KGAA004-2

Table S4 Sequences of siRNAs and shRNA

siRNA/ shRNA	Sense (5'-3')	Antisense (5'-3')
<i>siMYL5-1</i>	UCAACAAGGAGUACAUCAATT	UUGAUGUACUCCUUGUUGATT
<i>shMYL5-2</i>	GCUUCGCGCCGUAGUCUUATT	UAAGACUACGGCGCGAAGCTT
<i>siHIF-1α-1</i>	GGCCGCUCAAUUUAUGAAUTT	AUUCAUAAAUUGAGCGGCCTT
<i>siHIF-1α-2</i>	CCACCACUGAUGAAUUAATT	UUUAAUUCAUCAGUGGUGGTT

Table S5. Quantitative PCR primers for ChIP analysis

Primer set	Predicted binding		Reverse
	sites	Forward	
<i>MYL5 set-1</i>	GCGTG	AAAAAGTGCCCCTTCCTCTG	GAGGCTTTGTTCTCCCAAGG
<i>MYL5 set-2</i>	GCGTG	GCCATGAGGTCAGACGGG	TCTGCCAAGCACACTCTGTCT
<i>MYL5 set-3</i>	ACGTG	GAGGCCATGGTATAGTGGGG	CCGTCTGACCTCATGGCTG
<i>MYL5 set-4</i>	GCGTG	ACAGGACGAGGTGAGGGA	GAGGAAGGTTTCGGGATG
<i>HIF-1α P-1</i>	<i>AGCTCC</i>	CCTGCGTCGCTCGCCATT	GGTGATCCTCCTGTCCCCTCA
<i>HIF-1α P-2</i>	<i>AGCTCC</i>	GAACCCGCCTCCACCTCA	TGGCCGAAGCGACGAAGA